Dispersive analysis of πK scattering and resonances

A.Rodas

Based on:

J.R.Peláez and AR, Pion-kaon scattering amplitude constrained with forward dispersion relations up to 1.6GeV, Phys.Rev.D **93**, no. 7, 074025 (2016) [arXiv:1602.08404 [hep-ph]].,
J.R.Peláez, AR and J.Ruiz de Elvira, Strange resonance poles from $K\pi$ scattering below 1.8GeV, Eur.Phys.J.C **77**, no. 2, 91 (2017) [arXiv:1612.07966 [hep-ph]],
J.R.Peláez and AR, Work in preparation,

Universidad Complutense de Madrid

June 13, 2018

Index

Introduction

- Scalar octet $\rightarrow$ pseudo-Goldstone Boson.
- Lightest quark constituents.

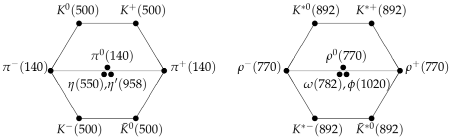

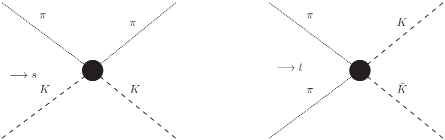

- Scattering $\Rightarrow$ Mandelstam variables $s = (p_1 + p_2)^2$, $t = (p_1 - p_3)^2$, $u = (p_1 - p_4)^2$.

Table of Content

Motivation

- πK scattering appears as final state in almost all hadronic strange processes.
- Examples: $B \to K^*(\to \pi K)\mu\mu$, D decays, CP violation

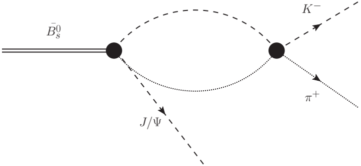

- π, K are pseudo-Goldstone Bosons of QCD $\Longrightarrow$ test of Chiral Symmetry Breaking
- Lowest energy test of SU(3) chiral dynamics $\Longrightarrow$ Scattering Lengths
- Strange resonances $\to$ spectroscopy $\to$ $K_0^*(800)/\kappa$
- Higher energies $\to$ Most resonances are not well determined, results come to be incompatible, pole vs Breit-Wigner definition.

Motivation

- UChPT $\rightarrow$ Good description in many previous works: Oller,Oset (1999).Dobado,Peláez (1997). Oller,Oset,Peláez (1999). Jamin,Oller,Pich (2000). Gomez Nicola,Peláez (2002).
- Experimental groups ask for simple but consistent parameterizations to be used at LHCb for CP violating processes.
- Also necessary for τ decays.
- Crossed channel $\pi\pi \rightarrow K\bar{K}$ first inelasticity of $\pi\pi$.
- Input in nucleon form factors, $g-2$ contribution etc...

Table of Content

Data: πK scattering

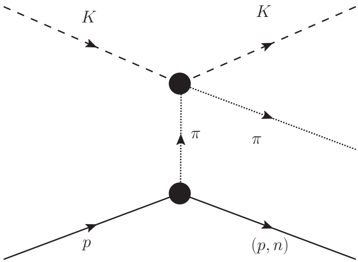

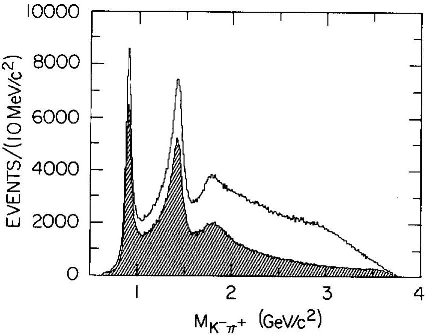

- 1.5×10^5 events used of $\approx 10^6$ total events collected.
- To extract scattering one has to extrapolate from $t < 0 \to t = m_\pi^2$, virtual $\pi \to$ real π.
- Good resolution and low momentum of the recoiling baryon.

Data: πK scattering

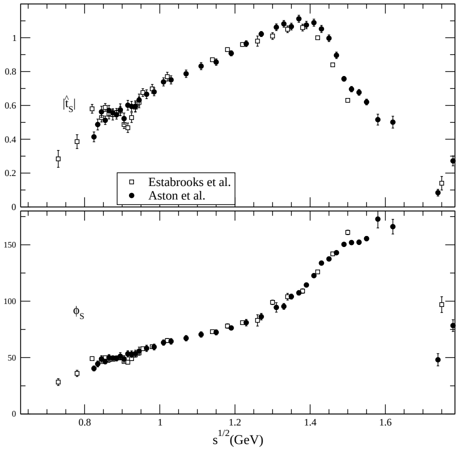

- LASS experiments from the $80's$, compatible in a big energy region $\rightarrow$ no systematics.
- Some incosistency close to the $K_0^*(800)$ region and at high energies.

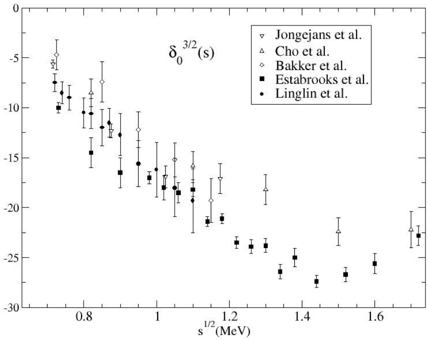

- Huge systematics → we need to select the correct solution.

Data: D^+ semileptonic decay

- Good control over electroweak vertex.
- $20k$ events.
- Compatible with production $\rightarrow$ huge uncertainties give no information.

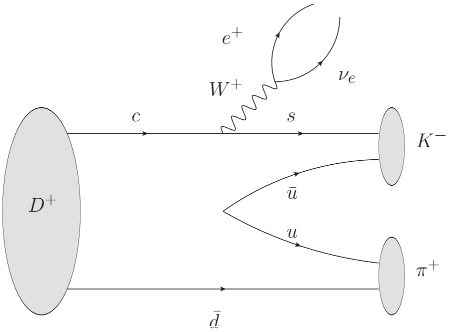

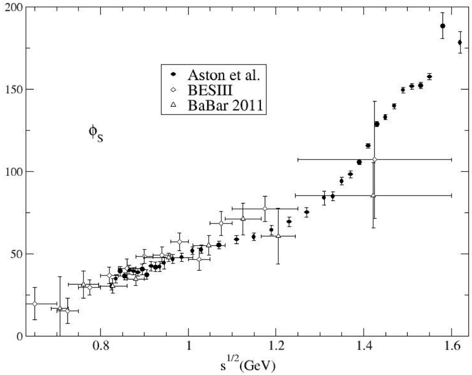

Data: D^+ and η_c decays

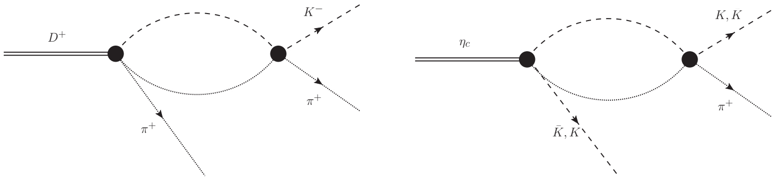

- New experiments.
- Data on the Dalitz much more precise.
- However, the determination relays on some models.

Data: final picture

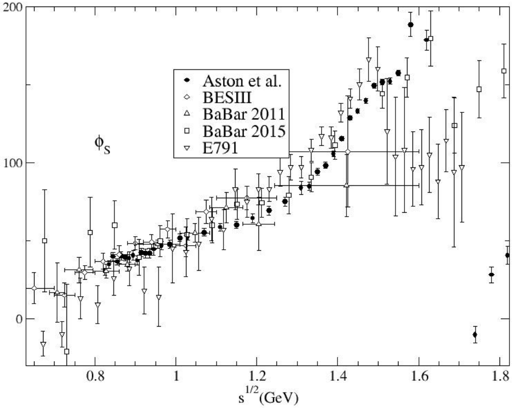

- Clearly incompatible with production.
- Analysis carried out in a too simple way (isobars, no unitarity implementation, big systematics...).
- Still low number of events ($10k$).

Data: $\pi\pi \to K\bar{K}$ scattering

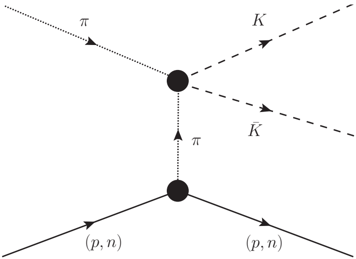

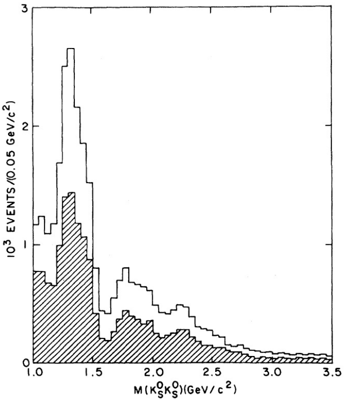

- Three main experiments done in the $80's$.
- None of them can separate the measurement of g_0^0 and g_2^0.
- Different systematic and contamination sources.

- Clearly incompatible.
- Only one of them is compatible with $\pi\pi$ scattering.
- Some data violates Watson's theorem.

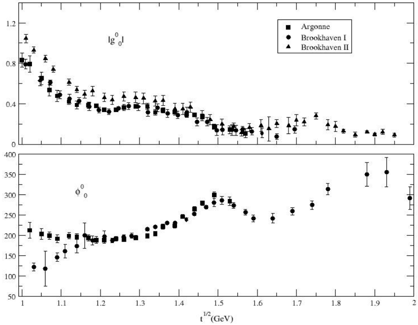

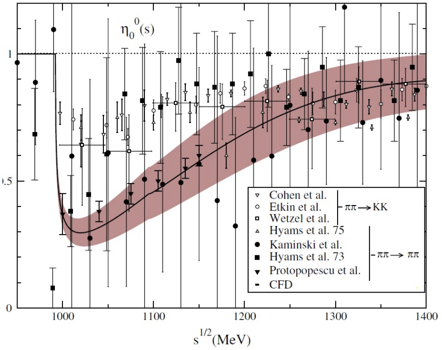

Table of Content

Scattering Lengths

- Two independent amplitudes I=1/2, 3/2.
- Can be written as a combination of a symmetric and antisymmetric amplitudes under $s \leftrightarrow u$ exchange.

$$T^{+}(s,t) = \frac{1}{3} T^{1/2}(s,t) + \frac{2}{3} T^{3/2}(s,t),$$
$$T^{-}(s,t) = \frac{1}{3} T^{1/2}(s,t) - \frac{1}{3} T^{3/2}(s,t).$$

- With the usual decomposition in partial waves

$$T^{I}(s,t) = 16\pi \sum_{\ell} (2\ell+1) t_{\ell}^{I}(s) P(z_s(t)),$$

with $z_s(t) = 1 + \frac{2t}{q^2(s)}$

- Scattering lengths

$$T^I(s_{th}, 0) = 8\pi m_+ a_0^I,$$

where $m_+ = m_\pi + m_K$

- At LO

$$a_0^- \propto \frac{1}{f_\pi^2} \qquad\qquad a_0^+ = \mathcal{O}(m_+^4).$$

- NLO $\longrightarrow$ LECs L_{1-8}

$$a_0^- \propto \frac{L_5}{f_\pi^4} \qquad\qquad a_0^+ \to 7L_i.$$

- NNLO $\longrightarrow 32C_i$, $a_0^- \to 10C_i$, $a_0^+ \to 23C_i$.

Scattering Lengths

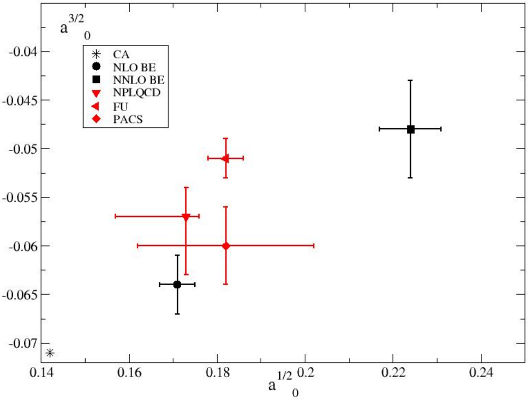

- Clear tension between Lattice Predictions and ChPT based calculations.
- SU(3) ChPT does not seem to be converging well.
- All of them compatible with the Unique measurement $\rightarrow$ DIRAC

Scattering Lengths

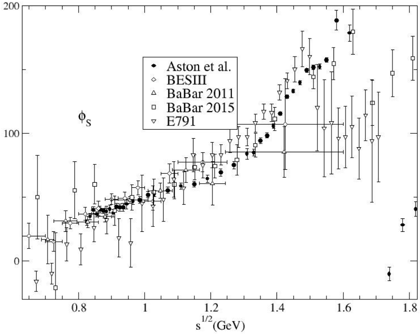

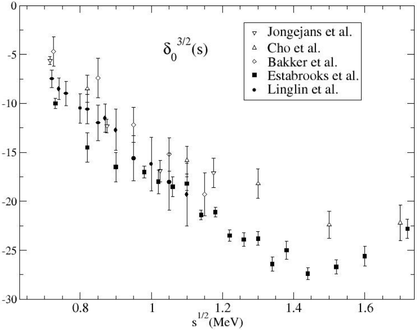

- Phenomenological analysis $\rightarrow$ scarcity of data at low energies.
- Huge systematic uncertainties lead to no information.
- Analiticity, crossing and unitarity need to be applied to get some predictability $\Rightarrow$ DISPERSION RELATIONS.

Table of Content

Dispersion relations

- UNITARITY $SS^\dagger = I \Rightarrow T - T^\dagger = TT^\dagger$.
- CAUSALITY $\Rightarrow$ ANALITICITY in first Riemann sheet $\Rightarrow$ resonance poles second Riemann sheet.
- ANALITICITY $\Rightarrow$ Cauchy theorem.

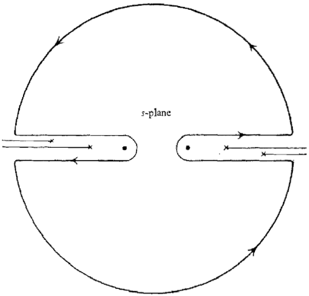

$$T(s,t) = \frac{1}{\pi}\int_{s_{th}}^{\infty} ds' \frac{T(s',t)}{s'-s} + LC.$$

Table of Content

FDR

- We will take for our analysis $t = 0$, they are called FDR.
- For the symmetric $s \leftrightarrow u$ amplitude one subtraction is needed

$$\mathrm{Re}\, T^+(s) = T^+(s_{th}) + \frac{(s - s_{th})}{\pi}$$
$$P\int_{s_{th}}^{\infty} ds' \left[\frac{\mathrm{Im}\, T^+(s')}{(s'-s)(s'-s_{th})} - \frac{\mathrm{Im}\, T^+(s')}{(s'+s-2\Sigma_{\pi K})(s'+s_{th}-2\Sigma_{\pi K})} \right],$$

where $\Sigma_{\pi K} = m_\pi^2 + m_K^2$.

- For the antisymmetric amplitude no subtraction is needed

$$\mathrm{Re}\, T^-(s) = \frac{(2s - 2\Sigma_{\pi K})}{\pi} P\int_{s_{th}}^{\infty} ds' \frac{\mathrm{Im}\, T^-(s')}{(s'-s)(s'+s-2\Sigma_{\pi K})}.$$

Unconstrained Fits (UFD):Elastic region

- We use the unitary functional form for the partial waves

$$t_l^I(s) = \frac{1}{\sigma(s)} \frac{1}{cot\delta_l^I(s) - i},$$

where $\sigma(s) = \frac{2q(s)}{\sqrt{s}}$ and

$$cot\delta_l^I(s) = \frac{\sqrt{s}}{2q^{2l+1}} \sum B_n \omega(s)^n,$$

- with $\omega(s) = \frac{\sqrt{y(s)} - \alpha\sqrt{y(s0) - y(s)}}{\sqrt{y(s)} + \alpha\sqrt{y(s0) - y(s)}}$ as our new variable (conformal mapping).
- Here $y(s) = (\frac{s - su}{s + su})^2$ defines the circular cut on the next figure.
- ω used to maximize the analyticity domain.

Unconstrained Fits (UFD):Elastic region

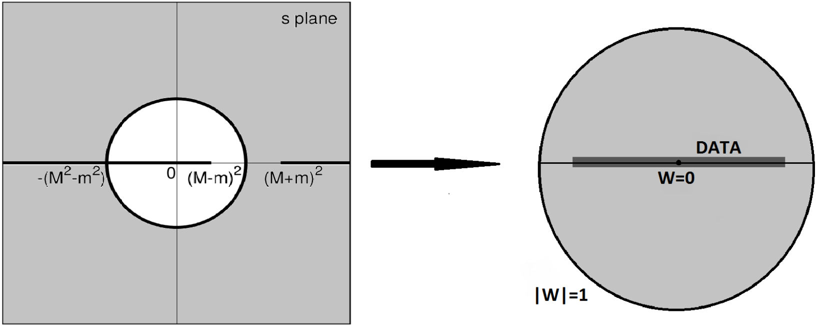

- Structure of the PW with different masses.
- α is used to center the point of energy s_c for the expansion.

Unconstrained Fits (UFD):Elastic region

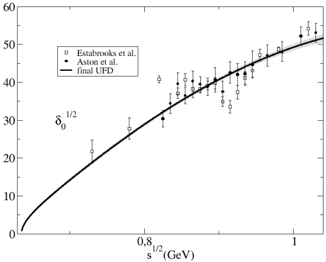

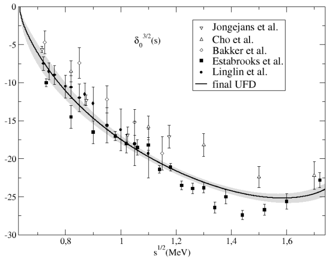

- $S^{1/2}$, $S^{3/2}$ and $P^{1/2}$ phase shifts, the I=3/2 is elastic in the entire region, while the others are only elastic below the $K\eta$ threshold.

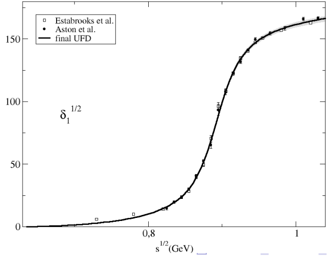

Unconstrained Fits (UFD):Inelastic region

- In the inelastic region $t_l^I = \frac{\eta_l^I(s)e^{2i\delta_l^I(s)}-1}{2i} = |t_l^I|e^{i\phi_l^I}$.
- We use complex rational functions that near each resonance look like BW.
- We impose matching conditions on the inelastic ηk threshold.
- We use up to $F^{1/2}$ which is very small and neglect $G^{1/2}$ in the studied energy region.
- Although we use for our analysis the $P^{3/2}, D^{3/2}$ and the $F^{1/2}$ their contribution is small. Not shown here.

Unconstrained Fits (UFD):Inelastic region

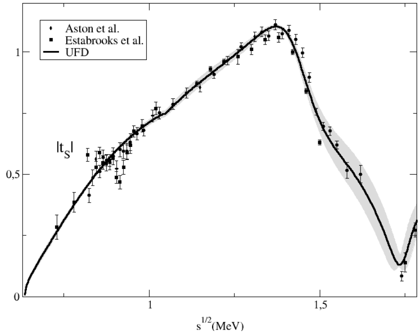

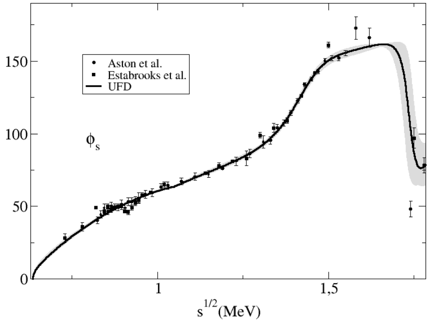

- Incompatibilities between Aston and Estabrooks sets of data.

- We construct tha amplitudes using the whole tower of partial waves.
- For $K\pi$ scattering we have two independent amplitudes $T^{1/2}$ and $T^{3/2}$, we study both combinations T^+ and T^-.
- Room for improvement $\rightarrow$ Constrained fits.
- Above $1.8 GeV$ the discrepancies are too big.

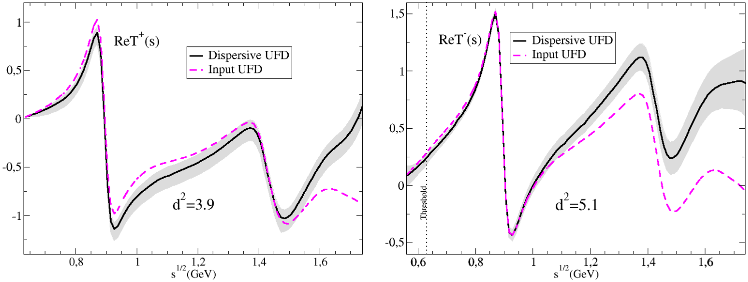

- The change in the symmetric amplitude around $1 - 1.2 GeV$ is caused by the change of the $S^{3/2}$-wave.
- The huge change of the antisymmetric one is caused by the Regge πK factorization constant.
- Now the amplitudes are fairly compatible with the analyticity requirements.
- The partial waves are now suitable to be used in our analysis.

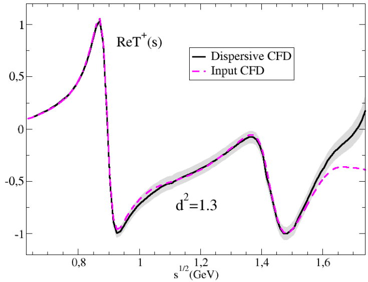

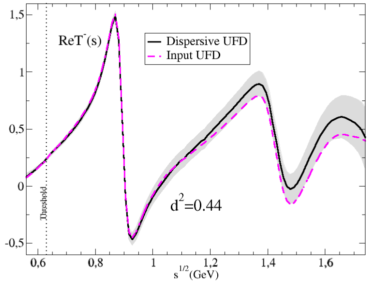

Constrained Fits

- $S^{3/2}$ clearly different from inital fit.
- Changes above that point, the CFD solution starts to be incompatible with the UFD.

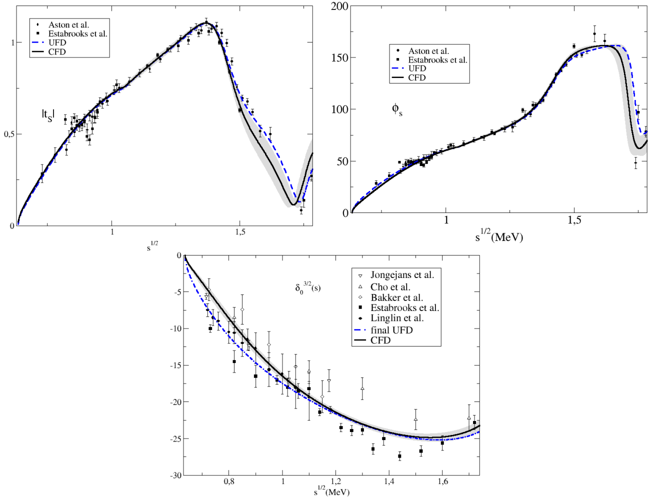

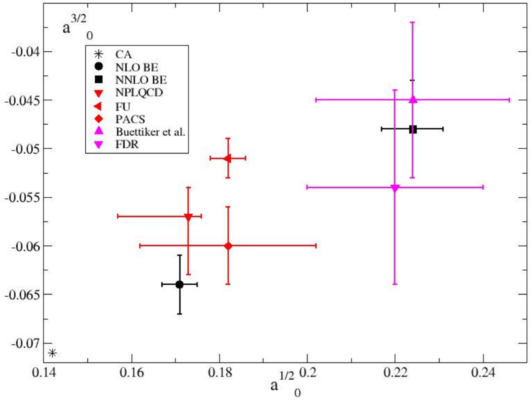

- Compatible with NNLO but no with Lattice.
- Allowed band in the a_0^- direction, a_0^+ bad predictability.
- a_0^+ cannot be imposed to determine a UNIQUE solution.
- Scarcity of data on $S^{1/2}$ do not help.

Table of Content

HDR

- Tension between FDR and Lattice.
- There is an universal band in the a_0^-, a_0^+ plane for $a_0^+ \Rightarrow$ no unique solution [Ananthanarayan et al. (2001)].
- Scattering lengths directly determined from scarcity of πK data.
- $K_0^*(800)$ pole out of FDR range of validity.

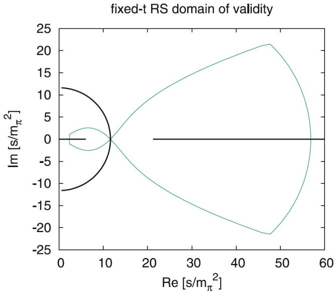

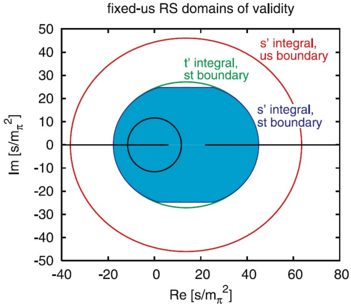

HDR

- We build dispersion relation with the relation $(s-a)(u-a)=b$.
- a fixed to maximize the region where they can be applied.
- Relation between $\pi K, \pi\pi, K\bar{K}$ to determine scattering lengths.
- Sub-threshold expansion $\Rightarrow$ Universal band not so universal.

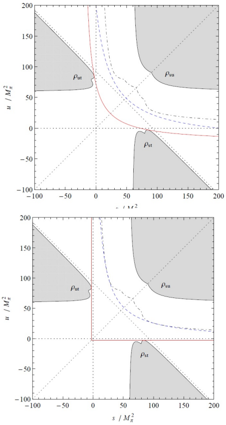

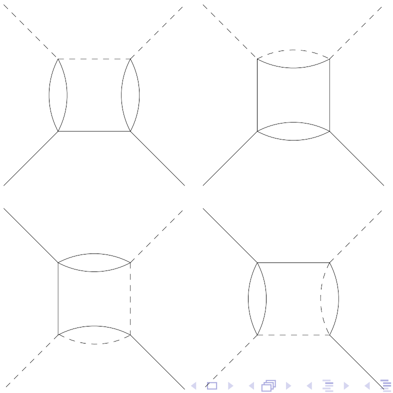

$\pi\pi \to K\bar{K}$

- Usual HDR for a crossed channel partial wave with one substraction

$$g_0^0(t) = \frac{\sqrt{3}}{2} m_+ a_0^+ + \frac{t}{\pi}\int_{4m_\pi^2}^{\infty} \frac{Img_0^0(t')}{t'(t'-t)} dt' +$$
$$\frac{t}{\pi}\sum_l \int_{4m_\pi^2}^{\infty} \frac{dt'}{t'} G_{0,2l-2}^0(t,t') Img_{2l-2}^0(t') + \sum_l \int_{m_+^2}^{\infty} ds' G_{0,l}^+(t,s') Imf_l^+(s')$$
$$= \frac{t}{\pi}\int_{4m_\pi^2}^{\infty} \frac{Img_0^0(t')}{t'(t'-t)} dt' + \Delta_0^0(t).$$

- $\Delta_0^0(t)$ contains the left cut. We can rewrite a dispersion relation for $g_0^0(t) - \Delta_0^0(t)$.
- We do not know the value of the partial wave $g_l^I(t)$ below $K\bar{K}$ threshold.
- The solution comes from the definition of the function $f_l^I(t) = \frac{g_l^I(t) - \Delta_l^I(t)}{\Omega_l^I(t)}$ with $\Omega_l^I(t) = e^{\frac{t}{\pi}\int_{4m_\pi^2}^{t_m} \frac{\phi_l^I(t')}{t'(t'-t)} dt'}$ applied to the previos function.

Omnès-Muskhelishvili problem

- The set of final Omnès-Muskhelishvili DR with as less subtractions as possible are

$$g_0^0(t) = \Delta_0^0(t) + \frac{t\Omega_0^0(t)}{t_m - t}\left[\alpha + \frac{t}{\pi}\int_{4m_\pi^2}^{t_m} dt' \frac{(t_m - t')\Delta_0^0(t')\sin\phi_0^0(t')}{\Omega_{0,R}^0(t')t'^2(t'-t)} + \frac{t}{\pi}\int_{t_m}^{\infty} dt' \frac{(t_m - t')|g_0^0(t')|\sin\phi_0^0(t')}{\Omega_{0,R}^0(t')t'^2(t'-t)}\right],$$

$$g_1^1(t) = \Delta_1^1(t) + \Omega_1^1(t)\left[\frac{1}{\pi}\int_{4m_\pi^2}^{t_m} dt' \frac{\Delta_1^1(t')\sin\phi_1^1(t')}{\Omega_{1,R}^1(t')(t'-t)} + \frac{1}{\pi}\int_{t_m}^{\infty} dt' \frac{|g_1^1(t')|\sin\phi_1^1(t')}{\Omega_{1,R}^1(t')(t'-t)}\right].$$

- Evaluating these DR with s real we recover the value of $|g_l^I(t)|$.

$\pi K \to \pi K$

- Simple integral equation, $\pi\pi \to K\bar{K}$ needed.

$$f_0^+(s) = \frac{m_+ a_0^+}{2} + \frac{1}{\pi}\int_{4m_+^2}^{\infty} \frac{Imf_0^+(s')}{s'(s'-s)} ds' +$$

$$\frac{t_b}{\pi}\sum_l \int_{4m_\pi^2}^{\infty} \frac{dt'}{t'} KG_{0,2l}^+(s,t') Img_{2l}^0(t') + \sum_l \int_{m_+^2}^{\infty} ds' K_{0,l}^+(s,s') Imf_l^+(s').$$

- We recover $\mathrm{Re}\, f_0^+(s)$ for real s.

$\pi\pi \to K\bar{K}$

- Both solutions come out to be compatible with HDR.
- Only solution B is compatible with $\pi\pi$ scattering $\Rightarrow$ favoured.
- Also favored From πK

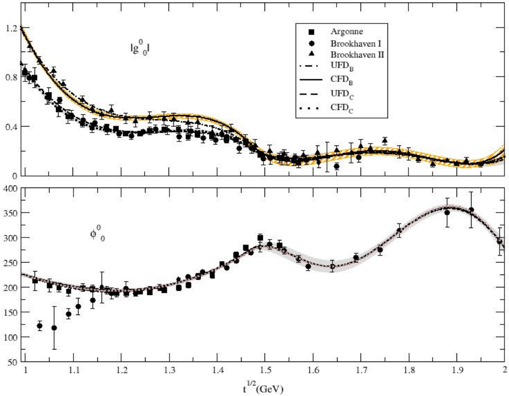

$\pi\pi \to K\bar{K}$

- Different $f_0(980)$ behaviors.
- Incompatible close to the $f_0(500)$ region.
- Sum rule coming from this channel predicts $a_0^- = 0.226 \pm 0.022$, not compatible with RS $a_0^- = 0.269 \pm 0.015$.

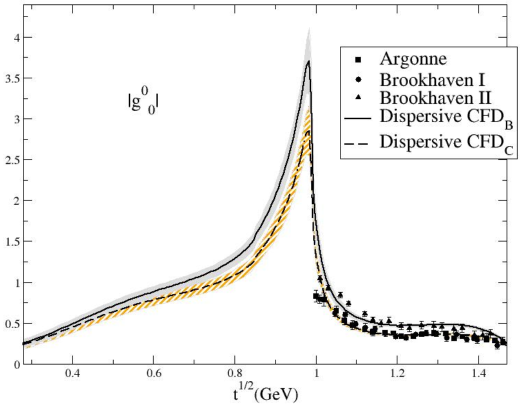

Scattering Lengths

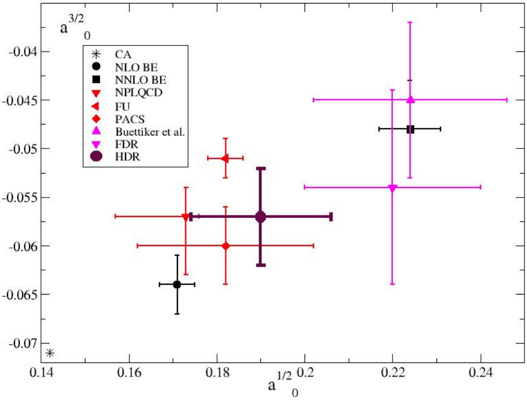

- PRELIMINARY RESULT FROM πK.
- Compatible with Lattice results.
- Solution still compatible with previous one due to the data.
- $a_0^- = 0.248 \pm 0.02$ compatible with previous sum rule.

Table of Content

Spectroscopy

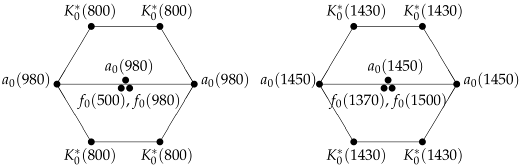

- We can study more then 6 resonances appearing in πK scattering.
- Precise determination using model independent techniques.
- Another 4 appearing in $\pi\pi \to K\bar{K}$ scattering.
- Some of the lightest strange and non-strange existing resonances.
- Can be used to determine $\Gamma(f_0(500) \to K\bar{K})$.

Spectroscopy for the κ particle

- Too broad to be determined using simple models.
- Threshold behavior (ChPT), Adler Zero and LHC play a role in its parameters.
- Problem shared by Lattice.

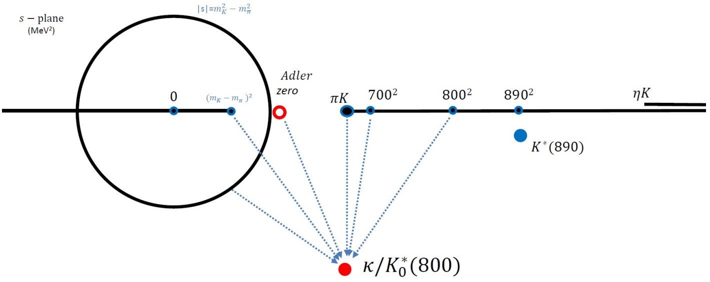

Spectroscopy for the κ particle

- Due to elastic unitarity

$$S^{II}(z) = \frac{1}{S^{I}(z)}.$$

- Looking for a zero of the scattering matrix in the first sheet.

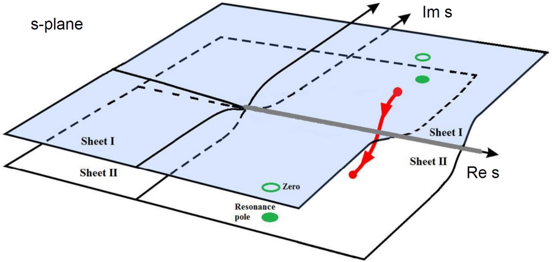

Spectroscopy for the κ particle

- Several different models and methods used to determine its parameters.
- Clear convergence with the use of dispersive techniques.
- Model dependent determinations not suitable for this scenario.

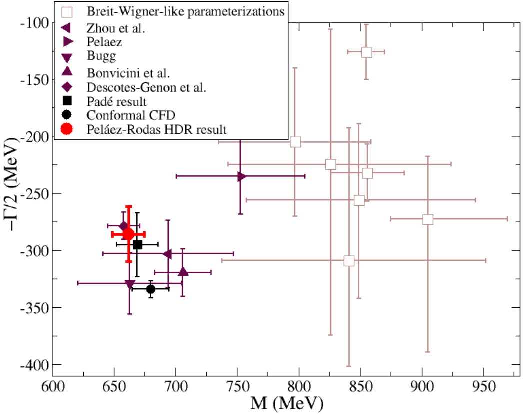

Spectroscopy for heavier resonances: Padés

- High L or wide resonance poles are not stable when calculated trough simple models.
- Usual $(q(s)/q(s_r))^L$ and $B_L(q, q_r)$ $\Rightarrow$ deviations in the width.
- Rigorous dispersive techniques cannot be applied at high energies (inelastic regions).
- The partial wave is described by a Padé approximant in the complex plane.

$$t_I(s) \simeq P_1^N(s, s_0) = \sum_{k=0}^{N-1} a_K (s - s_0)^k + \frac{a_N (s - s_0)^N}{1 - \frac{a_{N+1}}{a_N}(s - s_0)}.$$

- It is a model independent calculation. No specific functional form.
- No a priori relation between residue and pole position.
- The resonance may be surrounded by other non-analytic structures $\Rightarrow$ more poles have to be included inside our approximants.

- The method is suitable for the calculation of both elastic and inelastic resonances.
- The Padé sequence gives us the continuation to the continuous Riemann Sheet.
- This method was applied for the first time to study the σ and ρ resonances in P. Masjuan and J. J. Sanz-Cillero, Pade approximants and resonance poles, Eur. Phys. J. C **73** (2013) 2594 doi:10.1140/epjc/s10052-013-2594-4.

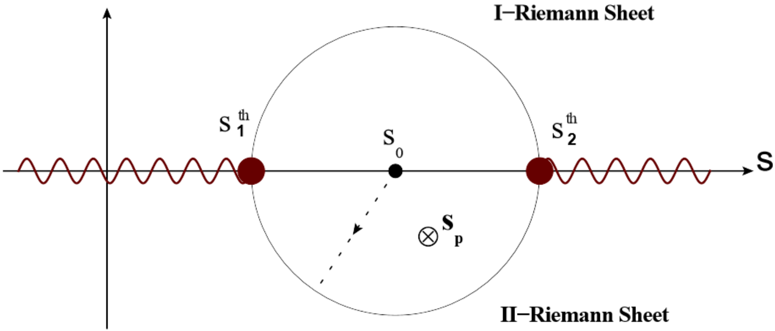

$K^*(892)$ as a test method

- The $K^*(892)$ is the simplest resonance that could be determined through padé approximants. Its parameters come out to be compatible with other determinations (pole) as it is a simple Breit-Wigner like resonance. $\sqrt{s_p} = (892 \pm 1) - i(29 \pm 1)$

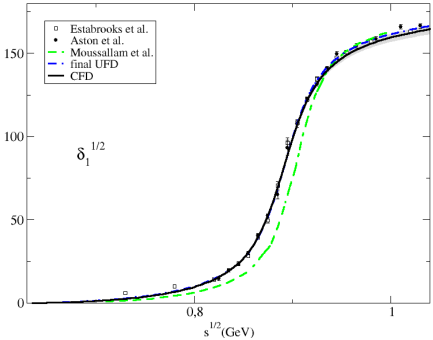

Figure: $P^{1/2}$ phase shift.

- First we obtain the difference between s_p^{N-1} and s_p^N for the whole energy region of the fit.
- Run a Montecarlo for every fit to calculate the statistical errors of every resonance.
- We stop at a N ($N+1$ derivatives) where the systematic uncertainty is smaller than the statistical one (usually $N=4$ is enough).
- For every fit we search the s_0 that gives the minimum difference between $N-1$ and N.

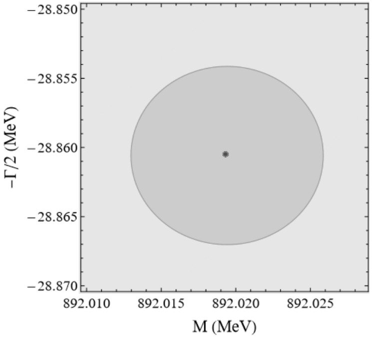

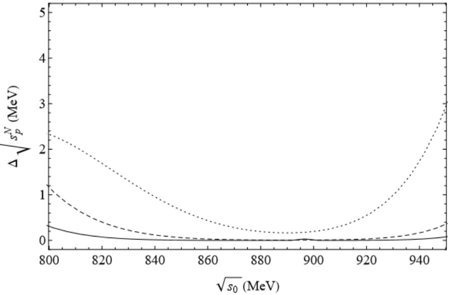

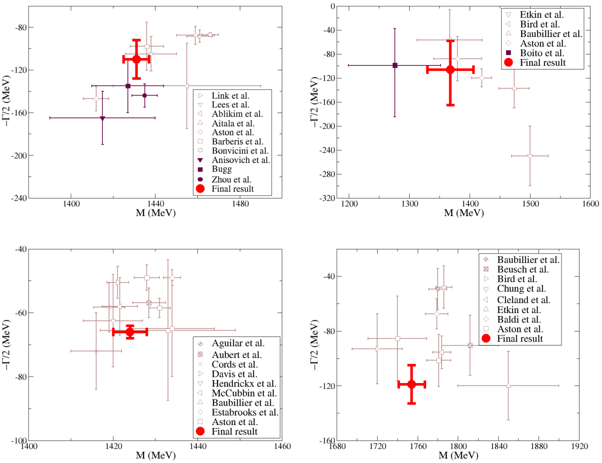

- Determinations of $K_0^*(1430)$, $K_1^*(1410)$, $K_2^*(1430)$ and $K_3^*(1780)$ vs PDG best values.

Table of Content

Khuri-Treiman analysis

- Already done for $D^+ \to \pi^+\pi^+K^-$ [Niecknig, Kubis (2015)].
- Using πK as input and predicting D^+ decay.

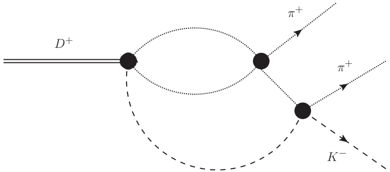

- Can we make it work the other way around η_c decay $\Rightarrow \pi K$ scattering.

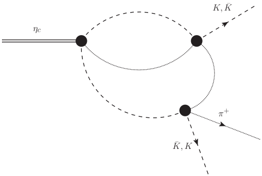

- New high precision LCHb/BELLE 2 data?
- KLF proposal?

Summary

- Dispersion relations impose a clear constrain when studying the data.
- Fixing some tension between different SL determinations.
- Provide a simple set of parameterizations that can be applied for other purposes.
- Useful to determine broad resonances $\rightarrow f_0(500), K_0^*(800)$.
- Simple method to study heavier resonances in a model independent way.
- **TO DO:**
- Finish combined analysis, obtain the poles of the $K_0^*(800), K^*(892)$.

Thank you for your attention!